ISBN: 978-3-95450-184-7 doi:10.18429/JACoW-IPAC2018-THPAK029

# STUDIES OF THE MICRO-BUNCHING INSTABILITY IN THE PRESENCE OF A DAMPING WIGGLER

M. Brosi*, J. Gethmann†, A. Bernhard, B. Kehrer, A. Papash,
P. Schönfeldt, P. Schreiber, J. L. Steinmann, A.-S. Müller
Karlsruhe Institute of Technology, Karlsruhe, Germany

*Abstract*

At the KIT storage ring KARA (KArlsruhe Research Accelerator), the momentum compaction factor can be reduced leading to natural bunch lengths in the ps range. Due to the high degree of longitudinal compression, the micro-bunching instability arises. During this longitudinal instability, the bunches emit bursts of intense coherent synchrotron radiation in the THz frequency range caused by the complex longitudinal dynamics. The temporal pattern of the emitted bursts depends on given machine parameters, like momentum compaction factor, acceleration voltage, and damping time. In this paper, the influence of the damping time is studied by utilizing the CLIC damping wiggler prototype installed in KARA as well as by simulations using the Vlasov-Fokker-Planck solver Inovesa.

## INTRODUCTION

The micro-bunching instability, a longitudinal instability, occurs for short electron bunches when their own electric field acts back on their longitudinal charge distribution. At the right conditions (e. g. bunch current, bunch length, momentum compaction factor and damping time), substructures form and lead to the emission of intense coherent synchrotron radiation (CSR) at wavelengths shorter than the bunch length. This radiation acts back on the bunch profile and creates a self-enhancing effect. This interaction can be described via the CSR impedance using the parallel plates model [1]. It was shown that by solving the Vlasov-Fokker-Planck equation with the parallel plates impedance as a perturbation in the Hamiltonian, the instability threshold [2, 3] and even the behavior of the instability above the threshold current is reproduced to a great extend [4]. By observing the emitted power of the synchrotron radiation, in the frequency range corresponding to the size of the substructures (at KARA in the THz range), the temporal development of the bunch profile due to the instability can be studied. The emitted synchrotron radiation spectrum directly depends on the longitudinal charge density and changes therefore with the rising and vanishing of substructures therein. The development of the temporal emission spectrum over the decreasing bunch current (Fig. 1) is reproducible for the same machine parameters and can therefore serve as a fingerprint for the machine state.

The micro-bunching instability has been studied at many light sources, e. g. ALS [5], Bessy II [6], DIAMOND [7]. At the KArlsruhe Research Accelerator (KARA) (the storage ring of the KIT light source fka ANKA), the dependency of the instability on multiple parameters, especially of its threshold current, has been studied in great detail before [3, 8, 9].

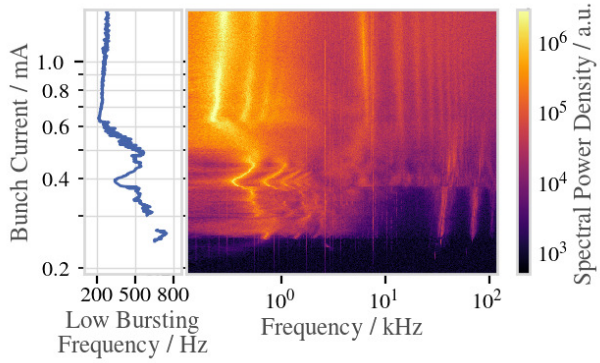


Figure 1: Fluctuation spectrogram of the emitted THz power. The fluctuations are caused by the instability and depend on the present machine settings. The left panel shows the extracted low frequency over bunch current corresponding to the repetition rate of the out-bursts in THz emission.

For this contribution, the influence of the longitudinal damping time on the behavior of the micro-bunching instability was studied using a prototype wiggler for the CLIC damping rings [10]. This superconducting wiggler (CLICDW) is in operation at KARA since 2016 [11]. It can be operated in the 2.5 GeV operation mode of KARA with a field of up to 2.9 T. Despite a strong vertical tune shift created by the wiggler, it can be operated with up to 2 T in KARA's 1.3 GeV operation mode, where the aforementioned micro-bunching instabilities can be observed. Its radiation causes an energy loss increase by 20 % which results in a faster damping. This damping can be utilized to study the influence of the damping time on the bursting behaviour.

## MEASUREMENT SETUP

For detailed studies of the instability behavior, precise measurements of the development of the emitted CSR power as a function of time as well as of the bunch currents are necessary. Therefore fast THz detectors, in this case Schottky barrier diode detectors from ACST [12] or VDI [13], are read-out with the in-house developed fast data-acquisition system KAPTURE [14]. This system samples and stores the detector pulse height (500 MHz) leaving out the noise during the 2 ns in-between pulses. With this combination of fast detectors and memory efficient read-out, the peak power of the THz pulse emitted from each bunch at every

* miriam.brosi@kit.edu
† gethmann@kit.edu

ISBN: 978-3-95450-184-7 doi:10.18429/JACoW-IPAC2018-THPAK029

Table 1: Machine Parameters

| Parameter | Value |
|---|---|
| Energy | 1.3 GeV |
| RF voltage | 771 kV |
| Filling pattern | mixed currents |
| Synchrotron frequency | 7.5, 7.7, 7.95 kHz |
| Horizontal tune | 0.7863 ± 0.0001 |
| Vertical tune | 0.7992 ± 0.0001 |

revolution is recorded at the "Infrared2" beam-line [15]. The bunch current was measured by combining the beam current measurement via DCCT with filling pattern measurement via time-correlated single photon counting (TCSPC) [16].

For each bunch, the measured THz peak power as a function of time gives the fluctuation spectrum of the THz emission caused by the momentary bursting behavior. The dependency of this behavior on the bunch current is made visible in the THz fluctuation spectrogram (Fig. 1) and shows characteristic features like the threshold current and the dominant frequencies, that show characteristic current-dependent changes for different machine settings. The low frequency (below 1 kHz) corresponds to the repetition rate of the sawtooth like outbursts in the THz emission. By extracting the low frequency from the spectrogram, as shown in the left panel, its dependency on current and settings of the CLICdw can be studied more easily.

The CLICdw is a superconducting wiggler with a fixed gap which means it does not change the geometric impedance like in-vacuum wigglers with permanent magnets would do. Its period length is $\lambda_w = 51.4$ mm and we were able to operate it with a magnetic field of $B_{wig} = 2$ T. This was the best trade-off between high field and stable machine parameters. Thus we operate with an undulator parameter [17] $K = 9.60$.

The optics we used is mainly optimized to provide a low momentum compaction factor and not a low beta function at the long straight sections where the CLICdw is located. So the simulated vertical beta function at this point is $\beta_y = (7.7 \pm 1.2)$ m. Together with the strong magnetic field of the wiggler, this shifts the vertical tune by 0.12. This tune shift needs to be compensated in order not to cross resonances that cause beam losses. Because KARA's current short bunch operation mode has tunes near 0.8, the compensation has to be done synchronously to the increase of the wiggler field. Due to the quadratic nature of the tune shift with the wiggler's field and the time delays of the field increase we were also limited in going to higher magnetic fields.

## MEASUREMENT

The storage ring quadrupoles are powered in five families. The individual powering is not forseen at present, not allowing local tune compensation. Hence, the optics was optimized not just to compensate the tune shifts, but also to minimize the maximum beta beat as well as the asymmetry of the beta functions. Though we only measured the tunes while optimizing the machine, we are quite confident,

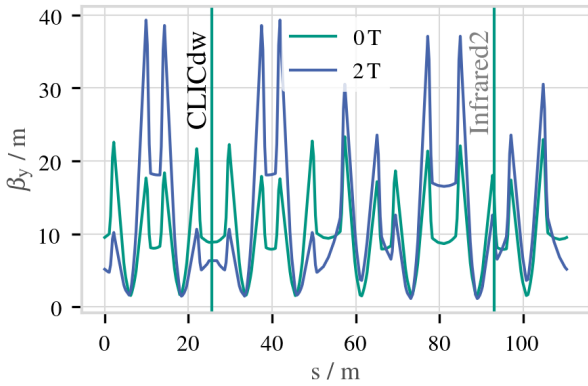


Figure 2: Simulated optics for 0 T and 2 T wiggler field. The beta functions are optimized using elegant [18].

that the optics is as "symmetric" as in the simulations and therefore the beta beat at the measurement point of the THz frequency ("Infrared2" in Fig. 2) is also relatively small. The optics optimization was done beforehand using elegant [18] and a LOCO [19] based model. Nevertheless, the beta functions are not completely compensated, as can be seen in Fig. 2.

With the help of the simulated optics the wiggler was ramped up step-wise to 2 T whilst the transverse tunes were measured with the bunch-by-bunch system *iGp12*, see e. g. [20], to an accuracy of $10^{-4}$. At each ramping step, the transverse tunes as well as the marginally changed synchrotron tune were corrected using the quadrupole families and the RF frequency if necessary. After this machine optimization we reproducibly achieved the setup summarized in Table 1.

Calculations using well-known equations [21] show that the momentum compaction factor only changes by $10^{-7}$which is negligible compared with the original momentum compaction factor of about $3 \times 10^{-4}$, therefore we did not put special efforts into compensating it at this time.

The measurements were done in separate fills (A - E). For the sake of completeness, the synchrotron frequency $f_s$ of fill A and B differs slightly from the others. With this set of fills we cover two cases—wiggler on and wiggler off—for the same range of bunch currents. Furthermore, fill C includes the transition from one case to the other as shown in Fig. 3.

## RESULTS

The THz fluctuation spectrograms for the cases with wiggler on or off show an overall similar appearance.

For example, the threshold $I_{th}$ of the instability, the current above which fluctuations in the emitted THz power occur, is the same for all fills (see Tab. 2, fill D did not reach low enough currents). That indicates, the CLICdw and therefore the longitudinal damping time has no significant influence on the threshold current. This is in agreement with the argument in [2] that the micro-bunching instability is a strong instability and hence its threshold should be independent from the damping time.The resulting approximation for the threshold (which is independent from the damping time) was

ISBN: 978-3-95450-184-7 doi:10.18429/JACoW-IPAC2018-THPAK029

Table 2: Bunch Current and Frequency at Instability Threshold

| Property | A | B | C | E |
|---|---|---|---|---|
| $B_{wig}$ / T | 0 | 0 | 0 → 2 | 2 |
| $I_{th}$ / µA | 217± 3 | 213± 3 | 215±2 | 220± 4 |
| $f_{th}$ / kHz | 30.9±0.3 | 30.1±0.3 | 29.6±0.3 | 29.7±0.3 |

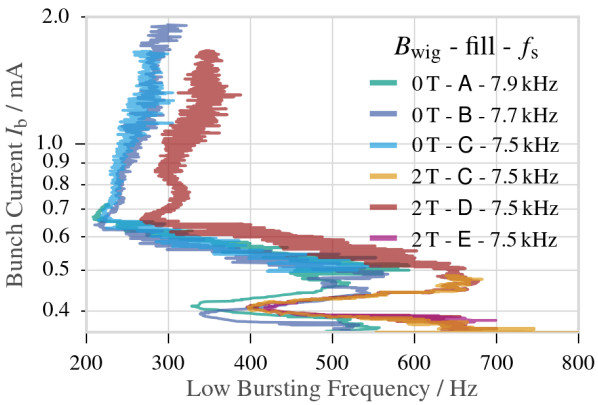


Figure 3: Low bursting frequency (periodicity of radiation outbursts as a function of bunch current for different fills. Shift in frequency visible for CLICDW at 0 T or 2 T.

proven to concur with measurements to a great extend in [3]. For the settings used in these fills, the simple scaling law predicts a threshold current of $I_{th} = 207\,\mu A$ for $f_s = 7.7\,kHz$.

Also, the fluctuations directly above the instability threshold have the same frequency $f_{th}$ (Tab. 2) and don't seem to be changed significantly by changes of the damping time.

The low frequency of the fluctuations in the emitted THz power (the periodicity of the radiation outbursts), however, shows a significant difference between the measurements with CLICDW on and CLICDW off. This low bursting frequency is displayed as a function of the bunch current in Fig. 3 for the different fills. For all fills the curves show similar features, like the kinks at approximately $(0.65 \pm 0.01)\,mA$ and $(0.40 \pm 0.01)\,mA$. Nevertheless, the curves for CLICDW off lie at lower frequencies whereas the ones with CLICDW on are shifted to higher frequencies. For example for a current of 0.8 mA the frequency is shifted from $(240 \pm 5)\,Hz$ to $(310 \pm 5)\,Hz$.

That these low bursting frequencies depend on the damping time is not unexpected as can be explained with a simple model of the longitudinal dynamics during the THz outbursts. The additional potential acting on the bunch is the convolution of the wake function and the bunch profile [22]. The shorter the bunch is the stronger this additional wake potential is acting on the bunch and driving the growth of substructures. These substructures lead to the emission of coherent synchrotron radiation above the vacuum chamber cut-off, which is visible as an outburst of THz radiation. Due to filamentation and diffusion the substructures are smeared out at a point in time, making the bunch longer. For a longer bunch the wake potential is significantly weaker and the bunch length is damped down until it is short enough to generate a strong wake potential leading again to the growth of substructures and another repetition of this cycle. Such a cycle is visible in the bunch length and the energy spread as a saw-tooth like pattern [23, 24].

The time span between two outbursts at a given bunch current $I_b$ consists of two parts. The first part, the rise time of the bunch length is caused by the occurrence and filamentation of the substructures. This time changes as a function of $I_b$. The second part is the time it takes to damp down the bunch length from its maximum to its minimum. On the one hand, this depends strongly on the longitudinal damping time and explains how the damping time affects the repetition rate of the outbursts. On the other hand, it depends on the minimal and maximal bunch length at $I_b$.

As the bunch length decreases with current also the interaction between the longitudinal charge distribution and the impedance changes. Therefore, the low bursting frequency can change as a function of bunch current even for a constant damping time as seen in Fig. 3. A faster damping results in a similar behavior, shifted to higher frequencies.

The dependency of the low bursting frequency on the longitudinal damping time was also simulated with the Vlasov-Fokker-Planck solver Inovesa [25]. Changing only the damping time while leaving all other parameters unchanged resulted in a qualitative agreement of the shift of the low frequency with that seen in the measurements.

## SUMMARY AND OUTLOOK

By using a prototype CLIC damping wiggler installed at the KArlsruhe Research Accelerator (KARA), the dependency of some key properties of the micro-bunching instability on the longitudinal damping time was studied.

No significant changes of the threshold current and the high frequency directly above the threshold were observed. The low bursting frequency, equivalent to the repetition rate of the outburst in CSR, however, significantly shifted when the CLICDW was ramped up from 0 T to 2 T.

This observation is supported by similar results with a Vlasov-Fokker-Planck solver.

## ACKNOWLEDGEMENT

We would like to thank M. Süpfle and Y.-L. Mathis for their support during the beam times at the IR2 beam line. This work has been supported by the German Federal Ministry of Education and Research (Grant No. 05K16VKA), the Helmholtz Association (Contract No. VH-NG-320). J. Gethmann acknowledges the support by the DFG-funded Doctoral School KSETA. M. Brosi, P. Schönfeldt, and J. L. Steinmann acknowledge the support by the Helmholtz International Research School for Teratronics (HIRST).

## REFERENCES

[1] M. Venturini and R. Warnock, "Bursts of Coherent Synchrotron Radiation in Electron Storage Rings: a Dynamical

ISBN: 978-3-95450-184-7 doi:10.18429/JACoW-IPAC2018-THPAK029

Model", *Phys. Rev. Lett.*, vol. 89, no. 22, p. 224802, Nov. 2002, doi: 10.1103/PhysRevLett.89.224802

[2] K. L. F. Bane, Y. Cai, and G. Stupakov, "Threshold studies of the microwave instability in electron storage rings", *Phys. Rev. ST Accel. Beams*, vol. 13, no. 10, p. 104402, Oct. 2010, doi: 10.1103/PhysRevSTAB.13.104402

[3] M. Brosi *et al.*, "Fast mapping of terahertz bursting thresholds and characteristics at synchrotron light sources", *Phys. Rev. Accel. Beams*, vol. 19, no. 11, p. 110701, Nov. 2016, doi: 10.1103/PhysRevAccelBeams.19.110701

[4] P. Schönfeldt, M. Brosi, M. Schwarz, J. L. Steinmann, and A.-S. Müller, "Parallelized Vlasov-Fokker-Planck solver for desktop personal computers", *Phys. Rev. Accel. Beams*, vol. 20, no. 3, p. 030704, Mar. 2017, doi: 10.1103/PhysRevAccelBeams.20.030704

[5] J. M. Byrd *et al.*, "Observation of Broadband Self-Amplified Spontaneous Coherent Terahertz Synchrotron Radiation in a Storage Ring", *Phys. Rev. Lett.*, vol. 89, no. 22, p. 224801, Nov. 2002, doi: 10.1103/PhysRevLett.89.224801

[6] M. Abo-Bakr, J. Feikes, K. Holldack, P. Kuske, and G. Wustefeld, "Coherent emission of synchrotron radiation and longitudinal instabilities", in Proc. PAC'03,Portland, USA, May 2003, pp. 3023–3025, doi: 10.1109/PAC.2003.1289801

[7] W. Shields *et al.*, "Microbunch Instability Observations from a THz Detector at Diamond Light Source", *Journal of Physics: Conference Series*, vol. 357, no. 1, p. 012037, 2012.

[8] M. Brosi *et al.*, "Studies of the Micro-Bunching Instability in Multi-Bunch Operation at the ANKA Storage Ring", in Proc. IPAC'17,Copenhagen, Denmark, May, 2017, paper THOBA1, pp. 3645–3648, doi: 10.18429/JACoW-IPAC2017-THOBA1

[9] M. Brosi *et. al*, "Systematic Studies of Short Bunch-Length Bursting at ANKA", in Proc. IPAC'16,Busan, Korea, May 2016, paper TUPOR006, pp. 1662–1665, doi: 10.18429/JACoW-IPAC2016-TUPOR006

[10] Y. Papaphilippou *et. al.*, "Conceptual Design of the CLIC Damping Rings", in Proc. IPAC'12,New Orleans, Louisiana, USA, May 2012, paper TUPCC086, pp. 1368–1370.

[11] A. Bernhard *et. al.*, "A CLIC Damping Wiggler Prototype at ANKA: Commissioning and Preparations for a Beam Dynamics Experimental Program", in Proc. IPAC'16,Busan, Korea, May 2016, paper WEPMW002, pp. 2412–2415, doi: 10.18429/JACoW-IPAC2016-WEPMW002

[12] Advanced Compound Semiconductor Technologies (ACST) GmbH, http://www.acst.de/.

[13] Virginia Diodes, Inc., http://vadiodes.com/.

[14] M. Caselle *et. al.*, "A Picosecond Sampling Electronic 'KAPTURE' for Terahertz Synchrotron Radiation", in Proc. IBIC'14,Monterey, CA, USA, 2014, paper MOCZB1, pp. 24–28.

[15] Y.-L. Mathis, B. Gasharova, and D. Moss, "Terahertz Radiation at ANKA, the New Synchrotron Light Source in Karlsruhe", *Journal of Biological Physics*, vol. 29, no. 2, pp. 313–318, Jun. 2003, doi: 10.1023/A:1024429801191

[16] B. Kehrer *et. al.*, "Filling pattern measurements using dead-time corrected single photon counting" in Proc. IPAC'18,Vancouver, Canada, April 29-May 4, 2018, paper WEPAL027, this conference.

[17] H. Wiedemann, "Particle Accelerator Physics", Berlin, Heidelberg, Germany: Springer, 2007, doi: 10.1007/978-3-540-49045-6

[18] Micheal Borland, "elegant: A Flexible SDDS-Compliant Code for Accelerator Simulation", Sep. 2000, http://www.aps.anl.gov/Accelerator_Systems_Division/Accelerator_Operations_Physics/manuals/elegant_latest/elegant.pdf

[19] J. Safranek, "Experimental determination of storage ring optics using orbit response measurements", *Nucl. Instr. Meth.*, vol. 388, no. 1–2, pp. 27–36, Mar. 1997, doi: 10.1016/S0168-9002(97)00309-4

[20] E. Hertle *et. al.*, "First Results of the New Bunch-by-bunch Feedback System at ANKA", in Proc. IPAC'14,Dresden, Germany, Jun 2014, paper TUPRI074, pp. 1739–1741, doi: 10.18429/JACoW-IPAC2014-TUPRI074

[21] R. P. Walker, "Wigglers", in Proc. CAS'95,Geneva, Sep.-Oct. 1995, pp. 807–835.

[22] J. B. Murphy, S. Krinsky, and R. L. Gluckstern, "Longitudinal wakefield for synchrotron radiation", in Proc. 16th Particle Accelerator Conference (PAC'95), Dallas, TX, USA, May 1995, pp. 2980–2982, doi: 10.1109/PAC.1995.505757

[23] K. L. F. Bane, and K. Oide, "Simulations of the longitudinal instability in the SLC damping rings", in Proc. PAC'93,Washington D.C., USA, May 1993, pp. 3339–3341.

[24] B. Kehrer *et. al.*, "Time-Resolved Energy Spread Studies at the ANKA Storage Ring", in Proc. IPAC'17,Copenhagen, Denmark, May 2017, paper MOOCB1, pp. 53–56, doi: 10.18429/JACoW-IPAC2017-MOOCB1

[25] P. Schönfeldt, M. Brosi, M. S. Schwarz, J. L. Steinmann, and A.-S. Müller, "Parallelized Vlasov-Fokker-Planck solver for desktop personal computers", *Phys. Rev. Accel. Beams*, vol. 20, no. 3, pp. 030704, Mar. 2017, doi: 10.1103/PhysRevAccelBeams.20.030704